AC/DC Converter Topologies Comparison for More Electric Aircraft Applications

Fatma A. Khera[12], C. Gerada[1], Serhiy Bozhko[1], Pat W Wheeler[1]
[1] Power Electronics, Machines and Control Research Group (PEMC), University of Nottingham, Nottingham, UK
[2] Electrical Power and Machines Engineering. Department, Tanta University, Egypt
E-mail: fatma.khera@gmail.com

***Abstract*—This paper compares the potential AC/DC power converter topologies that are appropriate for medium voltage and medium/high power aircraft applications. The power converter's rated power and the DC distribution voltage level in this application assumed to be 1MW and 3kV. The topologies explored include multi-level and modular converter structures that are connected in series and/or in parallel to achieve the rated power and DC-link voltage. The main aim of this research is to review the AC/DC converters topologies and then select the best candidate for the target application. The loss and efficiency of the converter topologies are determined based on available SiC semiconductor devices. Simulation results obtained using PLECs software are used to compare between different power converter topologies in terms of losses, weight, and power density to identify the best candidate.**

Keywords—AC/DC converter, medium voltage and medium/high power converters, aircraft applications and modular converter.

I. Introduction

In the last two decades, the aviation industry has been working on the more electric aircraft to reduce the CO2 emission (MEA) [1]. The features of the MEA are quiet, environmentally responsible, and energy-efficient [2, 3]. Currently, DC distribution voltages of 270V and 540V are widely employed and regarded as high-voltage DC (HVDC), but it is expected that the voltage level will enter the medium DC voltage range (kV) for future aircraft propulsion systems [4]. Using the medium DC voltage allows the distribution of power to increase from hundreds of KW to ones MWs. Higher voltage is therefore recommended in the electric power system (EPS) of the aircraft when propulsion systems are considered to reduce the current and hence cable diameter and cable weight [5].

One of the key components of the EPS of the aircraft is the AC electric machine, which can be used as a generator to power the EPS and also widely applied to drive different onboard loads. Working with medium voltage and medium/high power requires the use of multi three-phase machines for better machine power density, cooling system, and reliability (i.e., fault tolerance) [6-8]. Multiple three-phase machines have been used in various applications, particularly aerospace applications due to their fault tolerance and flexibility in providing different aircraft architecture designs [9].

The EPS requires AC/DC power electronic converters for interfacing to different electric machines that works as sources and loads [10]. Using multiple three-phase machines allows the using of technical building block (TBB) based converter structure where multiple AC/DC power converter units connected in series and parallel layouts can be deployed. These structures allow to use of multiple power converter units with low voltage and low current device ratings.

This paper provides the structure of the TBB based converter for 1MW rated power and 3kV DC distribution system which suitable for the future aircraft propulsion applications. The potential AC/DC power converters, which may be suitable, have been investigated. Then, a comparison between the converter candidates is provided to define the best choice. Simulation results for the selected topologies are presented with highlighting their advantages and limitations. Finally, the conclusions are drawn.

II. Technical Building Block Converter Concept

The concept of technical building block based converter depends on using small power converters units. By connecting the power converter units in series or/and parallel, the required current, voltage, and power levels can be attained. By that, the power converter features as modular and scalable structure with enabling a wide range of voltage and power.

For 3kV DC distribution voltage, the semiconductor devices that are mostly available at that voltage level, are IGBTs, which do not perform effectively at high switching frequency with high voltage ratings. SiC-MOSFET devices have widely penetrated in industrial applications. It is evident that SiC-MOSFET significantly exceed Si-IGBT devices in relation to switching performance by significantly reducing switching loss. SiC MOSFET devices are well established by SiC manufacturers, such as Cree and Microsemi, for voltage rating 650V and 1.2kV with different range of current rating. For higher voltage rating, some manufacturers, such as Hitachi and MITSUBISI, have produced SiC-MOSFET at 3.3kV but they are not commercially available.

The connection of the TBB based converter, which is shown in Fig. 1, is as follows: three modules are connected in parallel from the DC-side while the AC terminals are connected to three phases of the machine terminals, forming a three-phase converter unit. Then, the converter units are connected in series from the DC-side in order to withstand 3kV DC-bus voltage, where the DC-voltage seen by each converter depends on the number of series modules. The parallel connection has been also required leading to lower DC current shared by each

module. In this paper, two parallel branches of two series converter units are considered, as shown in Fig. 2.

Different structures of the converter modules with different number of series and parallel modules can be used which might improve converter performance. This is at the account of more complex control. Effect of different number of units is not the scope of this paper due to the limited space. The machine features permanent magnet multi-three-phase machine, where the machine has 4 groups of three-phase winding forming 12-phase machine.

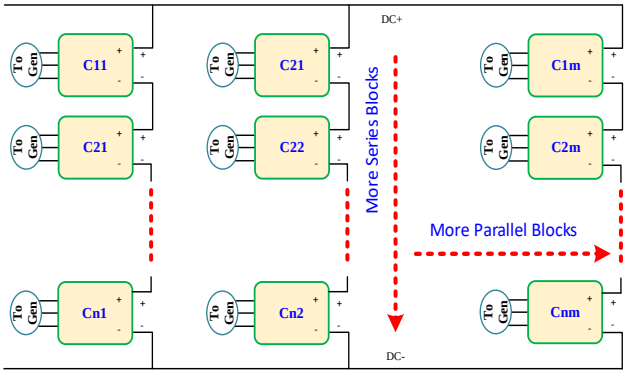

Fig. 1: Structure of TBB converter

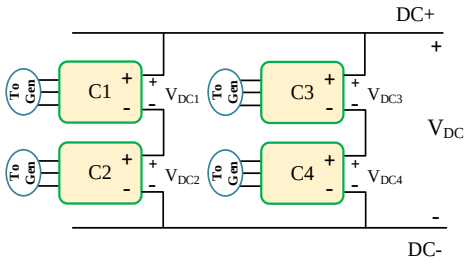

Fig. 2: TBB converter, two parallel branches of two series units

III. Converter Candidates

The main parameters, that need to be considered when selecting the type of the converter units shown in Fig. 2, are the DC-link voltage, fundamental frequency (machine electrical frequency) and the converter power. The selection of the power converters is restricted to the topologies that suitable for the medium voltage and medium/high power applications. The Preliminary description of the converter candidates will be introduced. These converters are two-level voltage source converter (2L-VSC), three-level neutral point clamped (NPC), three-level ANPC, T-type NPC, flying capacitor (FC) converter, and modular multilevel converter (MMC) [11-13].

A. 2-level voltage source converter

A 2L-VSC is composed of six active devices, as shown in Fig. 3. This structure is commonly used for low and medium voltage and power applications [13]. The converter structure and the control are considered straightforward. However, this converter suffers from high dv/dt in the output voltage, which could lead to failure of the insulation of the machine winding. It could also produce high harmonic distortion in the AC voltage and significant switching ripple in AC current leading to extra power loss. These issues can be solved by adding an LC filter between the converter and the machine. However, the use of the LC filter can increase the converter weight and consequently reduce power density.

To meet the specification of DC-bus voltage of 3kV, each unit should sustain DC-link voltage of 1.5 kV. So, the voltage stress of each device is 1.5kV and consequently devices with a voltage rating of 3.3kV should be used. Because the 3.3kV SiC MOSFETs are not commercially available, a series connection of 1.2kV devices can be used instead causing more complex layouts. Therefore, 2L-VSC has not been considered.

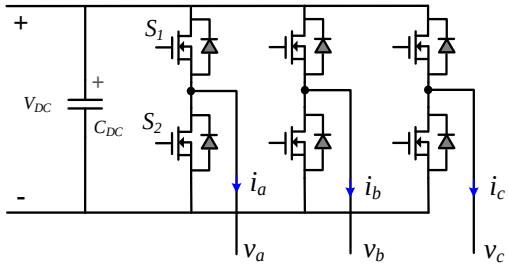

Fig. 3: 2L-VSC topology

B. Neutral point clamped (NPC) converter

Three-level NPC is composed of active devices, clamping diodes and DC-link capacitors, as shown in Fig. 4. This converter is widely used for medium voltage, high power drive applications. Compared to the 2L-VSC, the main advantage is the lower dv/dt, lower output voltage harmonics, and lower AC current switching ripple. Voltage balancing between DC-link capacitors are required due to deviation of neutral point voltage. This topology suffers from unequal distribution of power losses among the inner (S2 and S3) and the outer switches (S1 and S4). 3L-NPC requires half the voltage device rating compared to 2L-VSC and the switches are stressed by 750V, therefore 1.2kV SiC MOSFET can be used.

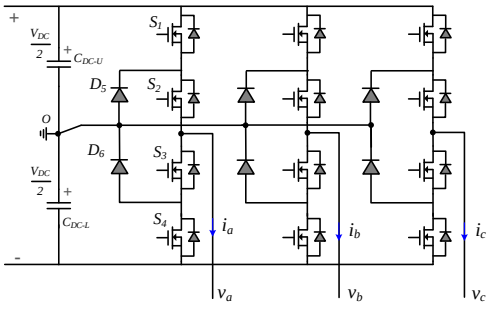

Fig. 4: Neutral point clamped (NPC) converter topology

C. Active neutral point clamped (ANPC) converter

Active NPC (ANPC) shown in Fig. 5, uses active devices in antiparallel to the clamping diodes in NPC converters to overcome the drawback of the unequal loss distribution. There are different methods that can be used to balance the loss

between the devices [14]. Similar to NPC, 1.2kV SiC MOSFETs devices, which are widely available in the market, can be used.

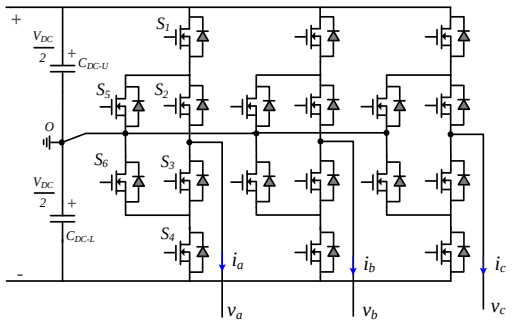

Fig. 5: Active neutral point clamped (ANPC) converter topology

D. T-type neutral point clamped (T-NPC) converter

T-NPC was proposed for drive applications. Instead of clamping diodes or switches in NPC and ANPC respectively, T-NPC uses a bidirectional switch to provide a controllable path to the current between the converter output terminal to the neutral-point of the DC link, as shown in Fig. 6. Compared to the NPC and ANPC topologies, this converter could provide a better efficiency and required the same number of devices with series connected switches for the main devices. 1.2kV SiC MOSFETs devices can be used.

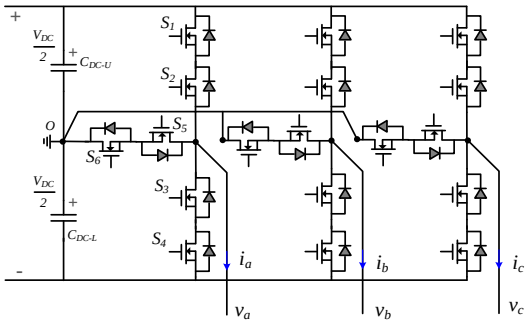

Fig. 6: T-type neutral point clamped converter (T-NPC) topology

E. Flying capacitor (FC) converter

The 3-level FC converter is similar to that of the NPC converter, where instead of using clamping diodes, the FC converter uses flying capacitors to clamp the switches to one capacitor voltage level. With this converter, it is important to balance the FC voltages and the complexity increases with increasing number of levels. FC converter requires more capacitors, which add to the converter's volume and weight and reduce its power density, therefore, it has been discarded.

F. Modular multilevel converter (MMC)

The MMC was originally used for HVDC transmission systems and also has gained more attention for use in the medium-voltage drives. The MMC phase consists of two arms. Each arm is formed by a series-connected identical sub-modules (SM), such as a half-bridge, full-bridge or other configurations, and an arm inductor. Each SM has a floating DC capacitor. It is important to balance the DC capacitor voltages and the complexity increases with increasing number of SMs. MMC is preferred to medium/high voltage applications, more than 10kVDC. Due to a large number of floating capacitors which of course increases the converter volume and weight of the converter, thus lower power density compared to the previous topologies, it has been excluded from this study.

G. H-bridge converter fed from isolated AC windings

The DC side series connection of H-bridge converter fed from isolated AC sources (open winding machine terminals) [13]. This converter has the advantage of relatively low voltage rated switches. Due to implementing only with open winding machine terminals, it has not been considered.

Table I provides a high-level comparison between the suggested topologies, in terms of voltage rating, current rating, and control complexity. According to the markets' availability of SiC MOSFET devices, NPC, ANPC, and T-NPC with 1.2kV voltage rating SiC MOSFETs have been selected. These converters have been compared in the following sections.

TABLE I: HIGH-LEVEL COMPARISON BETWEEN POWER CONVERTER CANDIDATES

Topology	Voltage rating	Current rating	Control Complex.	Comments
2L-VSC	High	High	Low	• Available in the market for different current range • EMI problem, high dv/dt
NPC	Medium	High	Medium	• Available in the market current level up to 150A • Loss unbalance
ANPC	Medium	High	High	• Available in the market • even loss distribution • Require additional active devices
T- NPC	Medium	High	Medium	• Available in the market • Use series connected devices
FC	Medium	High	High	• Large, distributed capacitors are required • Require additional capacitors
MMC	Medium	Low	High	• Large, distributed capacitors are required • Require additional capacitors
H-bridge	Low	High	High	• Isolated AC windings

IV. Modulation Semiconductor Loss and Cooling Requirement

The semiconductor loss, efficiency, device junction temperature and the requirements of cooling system have been calculated for the modular structure with the selected power converter topologies.

A. Semiconductor device loss

In this work, the machine electrical fundamental frequency is 2kHz. The switching frequency f_{sw} is set to 20 times of fundamental frequency, which is 40kHz. Due to working with quite high switching frequency, the SiC devices have been used. The semiconductor loss, conduction loss and switching loss, can be calculated using PLECS software thermal library. Depending on the datasheet parameters of the selected devices, the loss data can be extracted in shape of formulas or lookup tables at different junction temperatures and inserted into the PLECS thermal library. Some manufacturers, such as Cree, Microsemi, and Rohm [15], provide PLECS thermal model which can be directly applied.

The conduction loss of MOSFET can be calculated depending on the current direction and gate signal conditions. The MOSFET itself can be used to conduct the current from both directions. If the MOSFET has a positive gate signal, the MOSFET can conduct forward and reverse current; however, if the gate signal is zero/negative, the body diode can only conduct the reverse current as shown in Fig. 7.

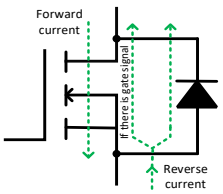

Fig. 7: Current directions in SiC MOSFET and its body diode

Therefore, when the gate signal is positive, the reverse current has two possible directions, the MOSFET channel at lower current level, or shared by the MOSFET channel and the body diode at higher current level. The sharing of the reverse current I_R between the MOSFET I_{DS} and the diode I_f is modelled by:

$$\begin{aligned} V_{DS} &= I_{DS} R_{DS-on} \\ V_{DS} &= V_{fo} + I_f R_f \\ I_R &= I_{DS} + I_f \end{aligned} \quad (1)$$

where V_{DS} is the voltage drop across the MOSFET. V_{fo} , and R_f donates the device threshold voltage (opening forward voltage drop at zero current), and on-state resistance of the diode, respectively. R_{DS-on} represents the MOSFET on-state resistance of the. These parameters can be easily obtained from the device characteristic curve from the datasheets. From equation (1), the current I_{DS} goes through the MOSFET causing voltage drop on R_{DS-on}. The current I_f stays zero until the V_{DS} exceeds V_{fo}. If I_R increases to a specific level, the current will flow through both the MOSFET and the diode.

The conduction power loss P_{Con} can be calculated by:

$$P_{Con} = V_{DS} I_{DS} \quad (2)$$

The switching loss is estimated during the on and off transition states of the semiconductor devices. The switching energies include turn-on energy loss E_{on} and turn-off energy loss E_{off} for the MOSFET and reverse recovery energy E_{rec} for of the body diode.

$$\begin{aligned} P_{SW-on}(t) &= f_{sw} \times E_{on}(\,|i(t)|) \times \frac{V_r}{V_n} \quad @i(t) > 0 \\ P_{SW-off}(t) &= f_{sw} \times E_{off}(\,|i(t)|) \times \frac{V_r}{V_n} \quad @i(t) > 0 \\ P_{SW-rec}(t) &= f_{sw} \times E_{rec}(\,|i(t)|) \times \frac{V_r}{V_n} \quad @\, i(t) < 0 \end{aligned} \quad (3)$$

where V_r is the voltage across the device during off condition and V_n is the semiconductor device test voltage which is obtained from datasheet. The switching characteristic curves for E_{on}, E_{off}, and E_{rec} versus current are given in the device datasheet at different device temperature.

The previous equations, (2) and (3), for the conduction and switching loss are also valid for the clamped diode in NPC converter, and it is known that the diode has only recovery loss.

B. Thermal requirements

Because of the semiconductor device loss, a thermal model is needed in order to estimate of the junction temperature of the semiconductor devices. The junction to case thermal impedance $R_{th\text{-}jc}$ is the inherent parameter of the semiconductor devices which cannot be controlled. The heatsinks are normally required to provide the pathway for heat to be well transferred away from the semiconductor devices to the surroundings. The heat transfer and the junction temperature can be controlled using different thermal impedance R_{th} of the heatsink.

Considering ANPC as an example and assuming each module (one-phase) is placed on one heatsink, therefore, there are six thermal resistors, as shown in Fig. 8. Ignoring the thermal impedance of the grease/paste $R_{th\text{-}ch}$, thus $T_h = T_c$, where T_h and T_c are heatsink and case temperature respectively. The required heatsink thermal impedance R_{th} and the junction temperature T_j for each device can be calculated by equations (4) and (5) respectively.

$$R_{th} = \frac{T_h - T_a}{P_{loss-total}} \quad (4)$$

$$T_j = P_{loss} \times R_{th-jc} + T_c \quad (5)$$

where P_{loss} is the device power loss and $P_{loss-total}$ is the total loss of devices placed on the same heatsink. The thermal capacitances are not taken into account due to working on a steady-state conditions.

The thermal resistance R_{th} of the heatsink is calculated in order to maintain the device with the highest power loss has maximum junction temperature less than or equal to 125ºC, at the ambient temperature T_a is 85ºC.

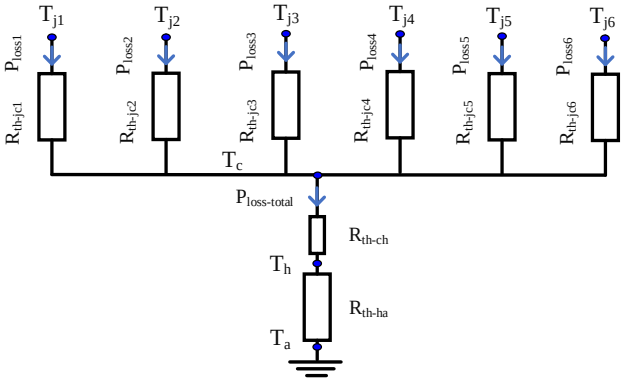

Fig. 8: Description of ANPC thermal resistance0s

V. Simulation Results

To compare between the three selected power converters as a basic unit of the configuration shown in Fig. 2, the simulations models were implemented using PLECS software for NPC, ANPC and T-NPC converters. The parameters used in the simulation models are given in Table II for the converter and machine sides. The rated power and the DC-bus voltage level are 1MW and 3kV respectively.

The SiC devices selection has a significant impact on the converter performances, since the power loss depends on the semiconductor conduction and switching parameters. SiC MOSFET module CAB530M12BM3 from Cree manufacturer and SiC diode module MSCDC450A120AG from microchip manufacturer, have been selected. Table III shows the specifications of the selected SiC devices.

Table II: Simulation Model parameters

Parameters	Value	Parameters	Value
DC-bus voltage	3 kV	Flux linkage	47mVs
Nominal rated power	1MW	Current RMS	196A
Number of phases	12	Pole pairs	4
Electrical frequency	2 kHz	Inductance	63µH
Switching frequency	40kHz	Phase resistance	0.012Ω
RMS Back electromotive force bEMF	410V	RMS Phase voltage	460V

Table III: SiC devices specifications

SiC Devices	MOSFET	Diode
Manufacturer	Cree	Microchip
Part number	CAB530M12BM3	MSCDC450A120AG
Voltage rating	1.2 kV	1.2kV
Current rating	540A @ 90 ºC	450A @ 90 ºC
Num. switches per module	2	2
Weight	300gm	300gm

Fig. 9 shows the average conduction and switching semiconductor power loss in kW for the converters working in generating (top) and motoring (bottom) modes. The results are for the selected converters NPC, ANPC, and T-NPC, at 100%, 75%, 50% and 25% of the rated power. It is clear that the conduction and switching loss for ANPC and T-NPC converters are approximately equal, and both are slightly lower than NPC converter. Fig. 10 shows the efficiency of the three converters in generating (top) and motoring (bottom) modes at 100%, 75%, 50% and 25% of the rated power. By lowering the load operating power from 100%, 75%, 50% to 25%, the efficiency increasing for the selected topologies. The efficiencies in the motoring mode are slightly lower than that in the generating mode for the three converters. The ANPC and T-NPC have the highest efficiency and NPC is slightly lower efficiency compared to ANPC and TNPC.

The thermal impedance R_{th} value determines the cooling system requirement. Table IV shows the required R_{th} value of the heatsinks for the three converter types at 100% rated power condition. It is considered that one heatsink is required for each phase. The thermal impedance is required to keep the maximum temperature of semiconductor devices doesn't not exceed the temperature limit ≤ 125ºC. ANPC requires the highest thermal resistance and consequently the best cooling system. The weight of heatsink should be kept as low as possible to maximise the power density. Calculating the exact weight of the heatsink considers quite difficult at this stage. Therefore, it is assumed that the heatsink factors (HSF) of 0.8, and 1.93 kg/kW are used to convert power loss to cooling system weight requirements. These two factors were calculated from two previous projects at University of Nottingham for NPC and ANPC. Table IV gives the calculated weight of the heatsink at the rated power condition for generating mode, and motoring mode is quite similar. The weight of the heatsink are close to each other for ANPC and T-NPC. The NPC requires the heaviest weight and the lowest power density.

On the basis of simulations results in terms of efficiency, and the requirements of the cooling system, and power density, the ANPC has been selected for prototype building and experimental work in the future work.

VI. Conclusions

This work introduced a preliminary description of the power converter candidates that are suitable for medium voltage and medium/high power aircraft applications. A high-level comparison between the different converter candidates was given, and the best options have been modelled for detailed comparison. The technical building block based converter was presented, in order to provide modular and scalable structure, where the selected converters are used as a basic block.

The semiconductor devices loss, efficiency and the cooling system of the different topologies using WBG technology, SiC devices, were obtained at different operating power in both generating and motoring modes. It has been found that the performance of ANPC and T-NPC are fairly similar, and both are slightly better than NPC. The cooling system required for ANPC is better than that required for NPC and T-NPC

topologies for all structures. The converter weight and power density in the different structures were determined. The power density of ANPC is the maximum which is slightly higher that T-NPC and NPC converters.

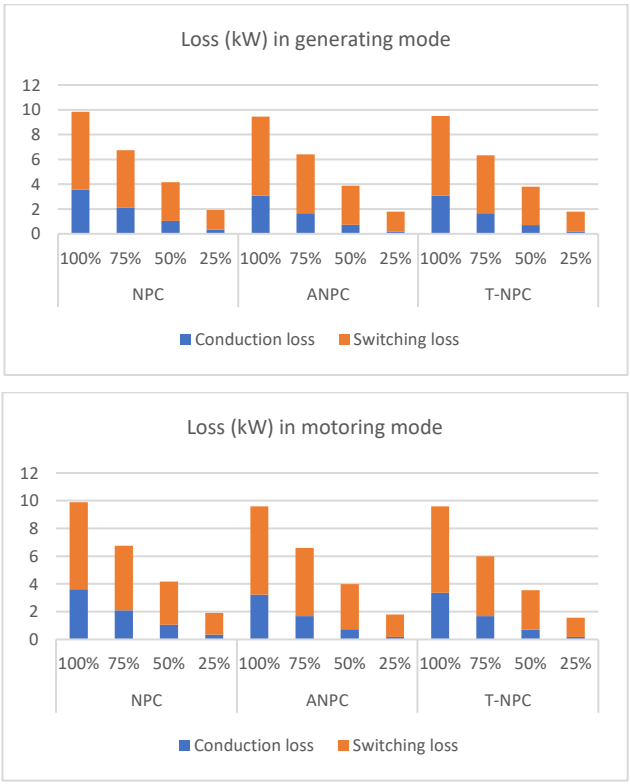

Fig. 9: Power loss (kW) at 100%, 75%, 50%, and 25% of Prated for generating and motoring modes

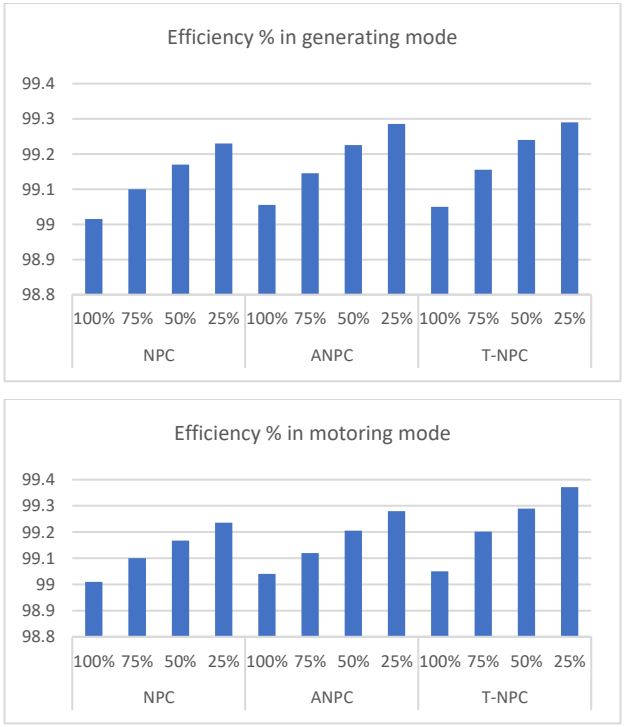

Fig. 10: Efficiency at 100%, 75%, 50%, and 25% of Prated for generating and motoring modes

Table IV: Thermal resistance and weight of the heatsink

	NPC	ANPC	T-NPC
Thermal resistance ^{o}C/W	0.0217	0.035	0.027
Weight (kg) @ HSF of 1.93 kW/kg	12.313	11.813	11.875
Weight (kg) @ HSF of 0.8 kW/kg	5.104	4.896	4.922

ACKNOWLEDGMENT

This research is being conducted in the frame of ORCHESTRA project, funding from Horizon 2020 under the European Union's Horizon 2020 research and innovation program.

REFERENCES

[1] https://www.airbus.com/en/innovation/zero-emission/electric-flight.
[2] C. L. Bowman, J. L. Felder, and T. V. Marien, "Turbo- and Hybrid-Electrified Aircraft Propulsion Concepts for Commercial Transport," in *2018 AIAA/IEEE Electric Aircraft Technologies Symposium (EATS)*, 2018, pp. 1-8.
[3] E. Sayed *et al.*, "Review of Electric Machines in More-/Hybrid-/Turbo-Electric Aircraft," *IEEE Transactions on Transportation Electrification*, vol. 7, no. 4, pp. 2976-3005, 2021.
[4] A. Trentin *et al.*, "Research and Realization of High-Power Medium-Voltage Active Rectifier Concepts for Future Hybrid-Electric Aircraft Generation," *IEEE Transactions on Industrial Electronics*, vol. 68, no. 12, pp. 11684-11695, 2021.
[5] P. Wheeler, "Technology for the more and all electric aircraft of the future," in *2016 IEEE International Conference on Automatica (ICA-ACCA)*, 2016.
[6] E. Levi, "Advances in Converter Control and Innovative Exploitation of Additional Degrees of Freedom for Multiphase Machines," *IEEE Transactions on Industrial Electronics*, vol. 63, no. 1, pp. 433-448, 2016.
[7] D. Golovanov *et al.*, "4-MW Class High-Power-Density Generator for Future Hybrid-Electric Aircraft," *IEEE Transactions on Transportation Electrification*, vol. 7, no. 4, pp. 2952-2964, 2021.
[8] A. El-Refaie and M. Osama, "High specific power electrical machines: A system perspective," *CES Transactions on Electrical Machines and Systems*, vol. 3, no. 1, pp. 88-93, 2019.
[9] M. v. d. Geest, H. Polinder, J. A. Ferreira, and M. Christmann, "Power Density Limits and Design Trends of High-Speed Permanent Magnet Synchronous Machines," *IEEE Transactions on Transportation Electrification*, vol. 1, no. 3, pp. 266-276, 2015.
[10] C. Klumpner and F. Khera, "EVALUATION OF INVERTER TOPOLOGIES FOR HIGH POWER/MEDIUM VOLTAGE AIRCRAFT APPLICATIONS," in *The 10th International Conference on Power Electronics, Machines and Drives (PEMD 2020)*, 2020, vol. 2020, pp. 188-193.
[11] S. Bozhko *et al.*, "Development of Aircraft Electric Starter–Generator System Based on Active Rectification Technology," *IEEE Transactions on Transportation Electrification*, vol. 4, no. 4, pp. 985-996, 2018.
[12] S. Mukherjee, S. K. Giri, and S. Banerjee, "A Flexible Discontinuous Modulation Scheme With Hybrid Capacitor Voltage Balancing Strategy for Three-Level NPC Traction Inverter," *IEEE Transactions on Industrial Electronics*, vol. 66, no. 5, pp. 3333-3343, 2019.
[13] B. W. a. M. Narimani, *High-power converters and AC drives*. Wiley-IEEE Press, 2017.
[14] T. Brückner, S. Bernet, and H. Güldner, "The Active NPC Converter and Its Loss-Balancing Control," *IEEE TRANSACTIONS ON INDUSTRIAL ELECTRONICS*, June 2005.
[15] https://www.plexim.com/download/thermal_models.